



# Acyl-CoA Thioesterase 1 (ACOT1) Regulates PPAR $\alpha$ to Couple Fatty Acid Flux With Oxidative Capacity During Fasting

Mallory P. Franklin,<sup>1</sup> Aishwarya Sathyanarayan,<sup>1</sup> and Douglas G. Mashek<sup>2,3</sup>

*Diabetes* 2017;66:2112–2123 | <https://doi.org/10.2337/db16-1519>

**Hepatic acyl-CoA thioesterase 1 (ACOT1) catalyzes the conversion of acyl-CoAs to fatty acids (FAs) and CoA. We sought to determine the role of ACOT1 in hepatic lipid metabolism in C57Bl/6J male mice 1 week after adenovirus-mediated *Acot1* knockdown. *Acot1* knockdown reduced liver triglyceride (TG) as a result of enhanced TG hydrolysis and subsequent FA oxidation. In vitro experiments demonstrated that *Acot1* knockdown led to greater TG turnover and FA oxidation, suggesting that ACOT1 is important for controlling the rate of FA oxidation. Despite increased FA oxidation, *Acot1* knockdown reduced the expression of peroxisome proliferator-activated receptor  $\alpha$  (PPAR $\alpha$ ) target genes, whereas overexpression increased PPAR $\alpha$  reporter activity, suggesting ACOT1 regulates PPAR $\alpha$  by producing FA ligands. Moreover, ACOT1 exhibited partial nuclear localization during fasting and cAMP/cAMP-dependent protein kinase signaling, suggesting local regulation of PPAR $\alpha$ . As a consequence of increased FA oxidation and reduced PPAR $\alpha$  activity, *Acot1* knockdown enhanced hepatic oxidative stress and inflammation. The effects of *Acot1* knockdown on PPAR $\alpha$  activity, oxidative stress, and inflammation were rescued by supplementation with Wy-14643, a synthetic PPAR $\alpha$  ligand. We demonstrate through these results that ACOT1 regulates fasting hepatic FA metabolism by balancing oxidative flux and capacity.**

During times of fasting, fatty acids (FAs) are released from adipose tissue and readily taken up by the liver, where they can be oxidized in the mitochondria via  $\beta$ -oxidation (1,2). To be transported into the mitochondria, FAs must be converted to acyl-CoAs by long-chain acyl-CoA synthetases (3).

A family of acyl-CoA thioesterases catalyze the reverse reaction—the hydrolysis of the fatty acyl-CoA thioester bond—resulting in the production of CoA and a free FA (4). This reaction seemingly removes acyl-CoAs from mitochondrial  $\beta$ -oxidation. In the liver, acyl-CoA thioesterase 1 (ACOT1) is the primary cytosolic thioesterase isoform (5). Peroxisome proliferator-activated receptor  $\alpha$  (PPAR $\alpha$ ) induces *Acot1* expression through a distal response element in the promoter region of the gene (6,7). However, fasting induces *Acot1* expression in whole-body *Ppara*-null mice and liver-specific *Ppara* knockout mice (6,7), suggesting that PPAR $\alpha$  is sufficient, but not necessary, for *Acot1* expression. Therefore, ACOT1 is speculated to be involved in FA trafficking during periods of increased hepatic FA influx and oxidation (8,9).

PPAR $\alpha$  is a transcription factor that governs the expression of genes involved in FA oxidation and is necessary to increase FA oxidative capacity during times of fasting (7). A wide variety of lipid species are speculated to serve as ligands for PPAR $\alpha$  activation, including free FAs (10–12). In addition to its role in FA oxidation, PPAR $\alpha$  promotes the expression of anti-inflammatory genes (13) and suppresses the expression of inflammatory genes (14). As such, PPAR $\alpha$  ligands are potential therapeutic agents for the prevention or treatment of inflammation (14).

Mitochondrial FA oxidation produces a mild amount of reactive oxygen species (ROS) at complexes I and III of the electron transport chain (15). This ROS production is balanced by antioxidant activity that protects the mitochondria from oxidative stress (16). During times of increased FA oxidation, however, increased membrane potential can cause a large amount of ROS to be produced,

<sup>1</sup>Department of Food Science and Nutrition, University of Minnesota, St. Paul, MN

<sup>2</sup>Department of Biochemistry, Molecular Biology and Biophysics, University of Minnesota, Minneapolis, MN

<sup>3</sup>Division of Diabetes, Endocrinology and Metabolism, Department of Medicine, University of Minnesota, Minneapolis, MN

Corresponding author: Douglas G. Mashek, [dmashek@umn.edu](mailto:dmashek@umn.edu).

Received 14 December 2016 and accepted 17 May 2017.

This article contains Supplementary Data online at <http://diabetes.diabetesjournals.org/lookup/suppl/doi:10.2337/db16-1519/-/DC1>.

© 2017 by the American Diabetes Association. Readers may use this article as long as the work is properly cited, the use is educational and not for profit, and the work is not altered. More information is available at <http://www.diabetesjournals.org/content/license>.

exceeding antioxidant capacity and leading to oxidative stress (15,17,18). Regulating the rate of FA oxidation in a cell is critical for minimizing ROS and oxidative stress that can occur during increased oxidation. Overexpression of ACOT1 in cardiomyocytes reduces FA oxidation and ROS production in mice with diabetic cardiomyopathy (19). These data suggest the potential involvement of ACOT1 in promoting oxidative capacity through substrate regulation and signaling. Despite high expression in the liver during fasting, the involvement of ACOT1 in lipid metabolism has yet to be characterized. Herein, we identify ACOT1 as a key enzyme that links FA flux and trafficking to PPAR $\alpha$  signaling, ROS, and inflammation.

## RESEARCH DESIGN AND METHODS

### Mouse Handling

The Institutional Animal Care and Use Committee of the University of Minnesota approved all protocols used in this study. Male C57Bl/6J mice, 7–9 weeks old, were purchased from Harlan Laboratories (Madison, WI) and housed in a vivarium with a controlled temperature (20–22°C) and light cycle (12-h light/12-h dark). Mice had free access to water and were fed a purified diet (TD.94045; Harlan Teklad, Madison, WI). One week before being sacrificed, mice received a tail vein injection of an adenovirus harboring either scramble short-hairpin RNA (shRNA), described previously (20), or shRNA targeted to *Acot1* mRNA. The *Acot1* shRNA adenovirus was generated from Open Biosystems (Huntsville, AL) based on accession number NM\_012006.2 (antisense sequence AAACACTCAC-TACCCAACACTGT). For the studies involving Wy-14643, mice were fed the purified diet supplemented with 0.1% Wy-14643 (Selleckchem, Houston, TX), a synthetic PPAR $\alpha$  ligand, for 7 days (21). An additional group of mice were fed a 45% high-fat diet (HFD; TD.06415) for 12 weeks before a tail vein injection of adenoviruses. One week after transfection, all mice were fasted overnight (16 h) and sacrificed unless noted otherwise.

### Hepatocyte Experiments

Pulse-chase studies with isotopes were conducted in primary hepatocytes isolated from mice fasted 16 h, as previously described (20,22). A Seahorse XF analyzer was used to determine total oxygen consumption rate (OCR) in primary hepatocytes isolated from control and *Acot1* knock-down mice after an overnight fast. Cells were seeded in collagen-coated XF cell culture plates at  $3 \times 10^4$  cells/well and incubated at 37° for 4 h. Media was changed to XF Assay media with 5.5 mmol/L glucose, 2 mmol/L GlutaMAX, and 1 mmol/L pyruvate and placed in a CO<sub>2</sub> chamber for an hour. Basal oxygen consumption was measured for 30 min, followed by an injection of either BSA control or 500  $\mu$ mol/L oleate, and OCR was determined for 30 min. Finally, antimycin A was injected at 1  $\mu$ mol/L to determine nonmitochondrial oxygen consumption. Average basal OCR and OCR in response to BSA control or 500  $\mu$ mol /L oleate was calculated.

### Triglyceride Hydrolase Activity

Tissues were lysed in a buffer consisting of 20 mmol/L Tris-HCl, 150 mmol/L NaCl, and 0.05% Triton X-100 (pH 8.0). Lysates were spun at  $15,000 \times g$  for 15 min. Infranatant was collected and mixed with 1,2-di-*O*-lauryl-rac glycerol-3-(glutaric acid 6-methylresorufin ester) and incubated at 30°C for 1 h. Kinetic readings were taken every 2 min at 530 nm excitation and 590 nm emission. Readings were compared with a standard curve generated with free resorufin.

### Metabolite Analyses

Serum  $\beta$ -hydroxybutyrate, tissue triglycerides (TGs), and tissue and serum FAs were analyzed as described previously (20).

### RNA Isolation and Analysis

mRNA was isolated from tissue or cells using Trizol reagent (Thermo Fisher Scientific, Waltham, MA), according to the manufacturer's protocol. cDNA was generated using SuperScriptVILO (Invitrogen, Carlsbad, CA). Quantitative real-time PCR was performed using SYBR Select (Thermo Fisher Scientific).

### Protein Preparation and Western Blotting

Protein was isolated from hepatocytes and liver tissue in lysis buffer and quantified by bicinchoninic acid assay. ACOT1 protein was determined by Western blotting using 80  $\mu$ g protein. Following SDS-PAGE, proteins were transferred to a polyvinylidene fluoride membrane and probed for ACOT1 with a custom antibody. The *Mus musculus* ACOT1/ACOT2 antibody was developed in rabbits by injecting the antigen CSVAAVGNTISYKDET-amide (21st Century Biochemicals, Marlboro, MA).

### ROS Determination

Cellular ROS and reactive nitrogen species (RNS) was determined using the OxiSelect In Vitro ROS/RNS Assay Kit (Cell Biolabs, Inc., San Diego, CA).

### Plasmids and Cloning

DsRed-Express N1 plasmid was purchased from Clontech (Mountain View, CA). *Acot1* cDNA was amplified from a pCMV6 *Acot1* plasmid purchased from Origene (Rockville, MD). *Acot1* cDNA was cloned into the multiple cloning site of DsRed-Express N1 by restriction enzyme digestion and T4 DNA ligase ligation. The S232A point mutation was achieved using a QuikChange site-directed mutagenesis kit from Agilent and previously reported primers (9).

### Cell and Tissue Imaging

Tissue sections were either frozen in Tissue-Tek O.C.T. (VWR, Eagan, MN) or fixed in 10% formalin and subsequently embedded in paraffin. Slides were deparaffinized and blocked in 3% BSA, incubated with ACOT1 antibody overnight, stained with DAPI, and mounted. Immunohistochemistry for Cd45 was determined, as were Oil Red O and hematoxylin-eosin (H-E) stains, by the University of Minnesota's Biological Materials Procurement Network Histology and Immunohistochemistry Laboratory. AML12 cells

were cultured in DMEM containing 10% FBS, 1% penicillin/streptomycin, and 0.1% insulin-transferrin-selenium solution. Cells were lipid-loaded overnight in serum-free DMEM with 500  $\mu\text{mol/L}$  oleate, then pretreated with 30  $\mu\text{mol/L}$  H89, a cAMP-dependent protein kinase (PKA) inhibitor, for 1 h before a 10-min treatment with 10  $\mu\text{mol/L}$  of 8-bromoadenosine 3',5'-cyclic monophosphate (8-Br-cAMP), a cell-permeable cAMP analog. Cells were fixed, stained for ACOT1 and with DAPI, and then mounted. COS7 cells were transfected using Effectene transfection reagent (Qiagen, Germantown, MD) with ACOT1-DsRed-Express. Cells were then treated and fixed as described for the AML12 studies.

### PPAR $\alpha$ Reporter Assays

COS7 or L cells were transfected with a PPAR $\alpha$  reporter construct (pSG5-GAL4-Ppar $\alpha$ ), firefly luciferase reporter plasmid (DK-MH-UASluc), control Renilla luciferase plasmid (pRLSV40), and empty DsRed-Express N1 plasmid, *Acot1*-DsRed-Express N1, or *Acot1*-S232A-DsRed-Express N1. Cells were treated in serum-free media with 500  $\mu\text{mol/L}$  oleate for 16 h, then treated with 8-Br-cAMP or vehicle for 6 h before being harvested for assessment of reporter activity using the Dual-Luciferase Reporter Assay System (Promega, Madison, WI). Firefly luciferase activity was normalized to Renilla luciferase activity.

### Thioesterase Activity Assay

Thioesterase activity was determined as previously described (23), with minor modifications. Frozen liver samples were homogenized with a dounce homogenizer for 15 s. Homogenates were centrifuged at 100,000g at 4°C for 1 h, and supernatants were collected. Samples were diluted in assay buffer (50 mmol/L KCl, 10 mmol/L HEPES), and 1 mg protein was loaded in each well. DTNB was added at a working concentration of 50  $\mu\text{mol/L}$  and read at 405 nm at 37°C. Palmitoyl CoA was added at 20  $\mu\text{mol/L}$  and read at 405 nm at 37°C for 3–5 min. CoA concentration as determined against a standard curve. Values were reported as nanomoles CoA per minute per milligram protein.

### Statistical Analysis

Values are expressed as means  $\pm$  SEMs. Statistical significance was determined using the Student *t* test or ANOVA, where appropriate.

## RESULTS

### ACOT1 Is Increased During Fasting

To assess the expression pattern and cellular distribution of ACOT1, we assessed mice that were fed or that were fasted for 16 h. As expected, fasting resulted in the induction of *Acot1* mRNA (Fig. 1A), which correlated to an increase in ACOT1 protein expression (Fig. 1B). Importantly, ACOT1 and ACOT2 are 93.7% homologous (24), and therefore the antibody generated for these studies recognizes both ACOT1 and ACOT2. However, ACOT2 is exclusively a mitochondrial protein (23), and previous groups have shown that ACOT2 runs below ACOT1 on SDS-PAGE gels (25). Therefore, to show the specificity of our

antibody, we compared our samples to those of mitochondrial preparations from mouse liver overexpressing *Acot2* (23). ACOT1 in liver lysates runs above ACOT2, as shown in Supplementary Fig. 1. ACOT2 is barely detectable in whole-liver lysates compared with ACOT1. During the fed state, ACOT1 exhibited low expression, but was robustly increased after 16 h of fasting. As such, our studies primarily focused on mice in the fasted state when ACOT1 is expressed. ACOT1 has been described as a cytosolic protein; however, to assess its cellular localization, we stained liver sections for ACOT1. As expected, ACOT1 was not present in the fed state but was abundant during fasting. Although ACOT1 was largely cytosolic, we observed ACOT1 in the nucleus in response to fasting (Fig. 1C), which was subsequently confirmed with Western blotting of nuclear fractions (Fig. 1D). This suggests a potentially undocumented nuclear role of ACOT1.

### *Acot1* Knockdown Reduces Fasting Liver TGs by Enhancing TG Turnover and Increases Oxidation of Endogenous and Exogenous FAs

To determine the contribution of ACOT1 to hepatic energy metabolism, we used adenovirally delivered shRNA to knock down *Acot1* in the liver. Seven days after transduction, control mice (cont. shRNA) or liver *Acot1* knockdown mice (*Acot1* shRNA) ( $n = 7$ –9 mice) were fasted for 16 h before being sacrificed. We observed a significant reduction ( $\sim 60\%$ ) in both *Acot1* mRNA (Supplementary Fig. 2A) and protein ( $\sim 60\%$ ) (Supplementary Fig. 2B). Immunohistochemistry exhibited reduced cytosolic and nuclear ACOT1 with *Acot1* knockdown (Supplementary Fig. 2C). This reduction in ACOT1 expression correlated to reduced thioesterase activity (Supplementary Fig. 2D).

*Acot1* knockdown significantly reduced hepatic TG content as determined by enzymatic assays and imaging of lipid droplets in H-E- and Oil Red O-stained liver sections (Fig. 2A and B). *Acot1* knockdown had no effects on liver lipid droplet accumulation in fed mice, consistent with its low expression in the fed state (Supplementary Fig. 3A). The reduced liver TGs observed in response to *Acot1* knockdown could arise from a reduction in de novo lipogenesis and/or TG synthesis, enhanced TG secretion in the form of VLDL, or enhanced TG breakdown and FA oxidation. Thus, we assessed each of these possibilities to determine which pathway(s) was altered and thereby led to reduced hepatic TG content in response to *Acot1* knockdown.

To assess de novo lipogenesis and TG synthesis, we performed radiolabel experiments in primary hepatocytes isolated from mice transduced with scramble control or *Acot1* shRNA adenoviruses. We incubated cells with [ $^{14}\text{C}$ ]acetate or [ $^3\text{H}$ ]glycerol for 2 h and measured incorporation of the label into the TG fraction. Rates of incorporation of either acetate or glycerol into the TG fraction were similar among treatment groups (Supplementary Fig. 4A and B), suggesting that de novo lipogenesis and TG synthesis are unaffected by *Acot1* knockdown. *Acot1* knockdown had little effect on serum TG (Supplementary Fig. 4C) or hepatic TG

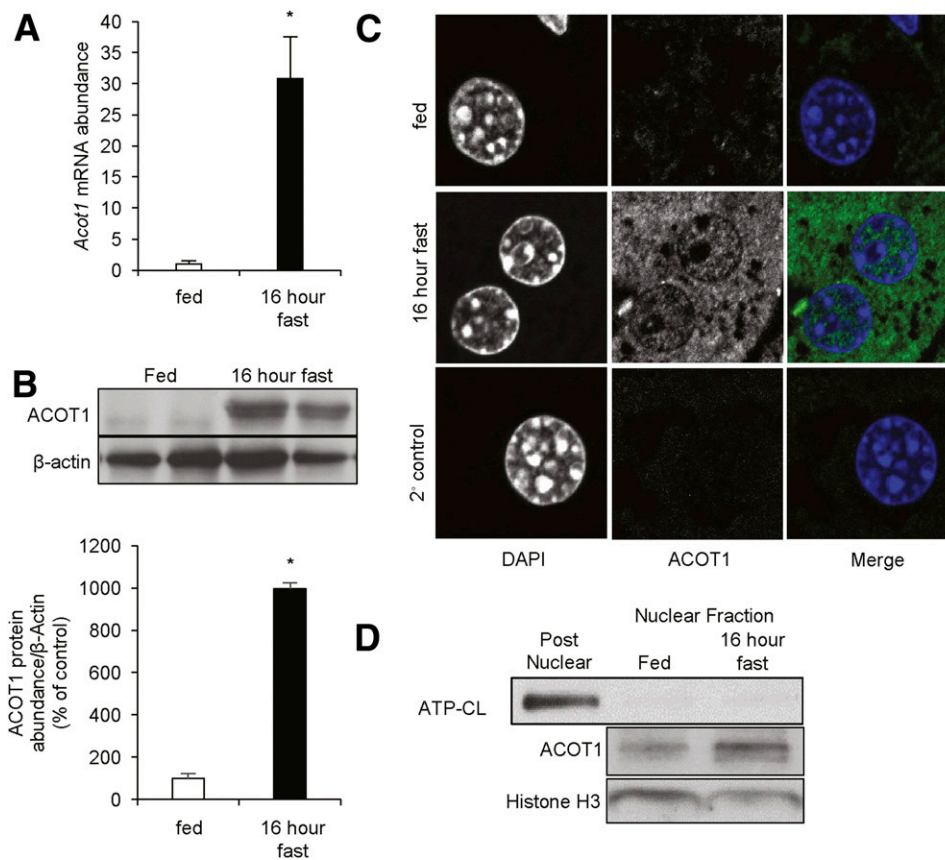


**Figure 1**—Hepatic ACOT1 is increased during fasting. C57Bl/6J mice were either fed or fasted overnight (16 h). *A*: *Acof1* expression was increased with fasting, as analyzed by RT-PCR ( $n = 5$  mice). *B*: Western blotting (top) and densitometry (bottom) of ACOT1 in fed and fasted mice. *C*: Fixed liver sections from fed or fasted (16 h) mice were probed with the ACOT1 primary antibody and Alexa 488 secondary antibody. *D*: Western blots of nuclear preparations from fed and fasted mice. \* $P < 0.05$ . ATP-CL, ATP-citrate lyase.

secretion based on serum TGs from animals treated with tyloxapol (Supplementary Fig. 4D), suggesting no change in VLDL secretion. These results were confirmed with radiolabeling studies in primary hepatocytes, which showed that *Acof1* knockdown had no effect on secreted TGs (Supplementary Fig. 4E). Together, these data suggest that changes in de novo lipogenesis, TG synthesis, or VLDL assembly and secretion are unaffected by *Acof1* knockdown. We next tested the effects of *Acof1* knockdown on TG hydrolysis. TG hydrolase activity significantly increased in tissue homogenates from livers treated with *Acof1* shRNA compared with control livers (Fig. 2C). Enhanced lipolysis paralleled an increase in serum  $\beta$ -hydroxybutyrate (Fig. 2D), indicative of enhanced FA oxidation. We again confirmed that these effects were specific to the fasted state because *Acof1* knockdown did not alter  $\beta$ -hydroxybutyrate in fed mice (Supplementary Fig. 3B). These data support a role for ACOT1 in mitigating the flux of acyl-CoAs to mitochondrial  $\beta$ -oxidation in the fasted state. To further assess alterations in FA flux, in vitro pulse-chase experiments were performed. Similar to the unchanged TG synthesis from acetate or glycerol (Supplementary Fig. 4A and B), incorporation of [ $^{14}$ C]oleate into the cellular TG pool was similar

among treatment groups (Fig. 2E). Consistent with increased TG hydrolysis in livers from *Acof1* knockdown mice, turnover of [ $^{14}$ C]TGs was significantly greater with *Acof1* knockdown in primary hepatocytes (Fig. 2F). In addition, FA oxidation was significantly increased in both the pulse (Fig. 2G) and chase periods (Fig. 2H) in the *Acof1* knockdown hepatocytes.

We next assessed OCR in primary hepatocytes from control and *Acof1* knockdown mice using a Seahorse XF analyzer. As expected, *Acof1* knockdown hepatocytes exhibited a significant increase in OCR with the addition of FAs compared with BSA control (Supplementary Fig. 5); although basal rates were numerically higher, they did not reach significance. To confirm the enzymatic importance of ACOT1 in regulating FA oxidation and TG turnover, we next transfected L cells with an empty DsRed-Express N1 vector (EV), *Acof1* DsRed-Express N1 (*Acof1*), or a catalytically dead mutant *Acof1*-S232A-DsRed-Express N1 (*Acof1* S232A) and performed a pulse-chase with [ $^{14}$ C]oleate. Expression and thioesterase activity of these mutants were confirmed (Supplementary Fig. 6). Cells transfected with *Acof1* exhibited less FA oxidation and more TG retention (Supplementary Fig. 7) than the EV and the *Acof1* S232A

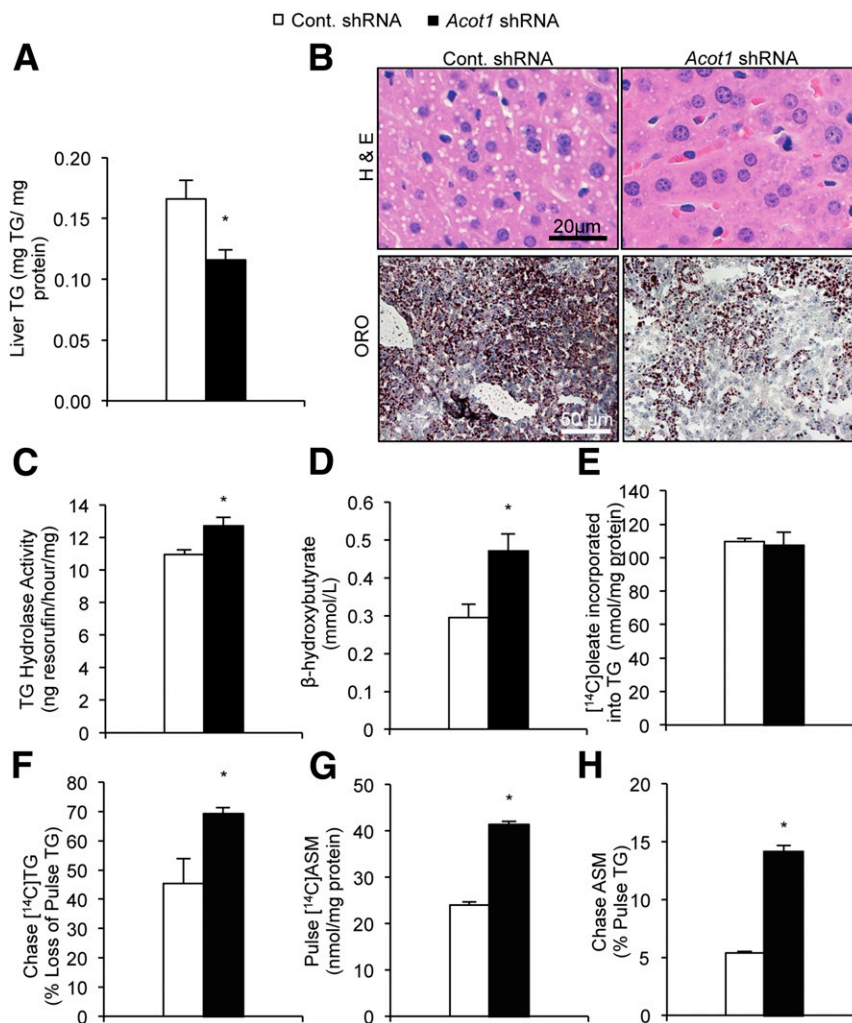


**Figure 2**—*Acot1* knockdown increases hepatic FA oxidation. *A*: *Acot1* knockdown reduced hepatic TGs. *B*: H-E and Oil Red O (ORO) stains of liver tissue showed fewer lipid droplets in the *Acot1* shRNA treatment group ( $n = 7-9$  mice). *C*: TG hydrolase activity was increased in liver tissue homogenates of mice treated with *Acot1* shRNA ( $n = 4$  mice). *D*: Serum  $\beta$ -hydroxybutyrate was increased after hepatic *Acot1* knockdown in mice fasted for 16 h. *E*: *Acot1* knockdown did not influence [ $^{14}$ C]oleate incorporation into cellular TGs. *F*: TG turnover as measured by [ $^{14}$ C]TG loss during the chase period was increased in response to *Acot1* knockdown. *Acot1* knockdown increased the oxidation of exogenous (*G*) and endogenous (*H*) FAs, as measured by [ $^{14}$ C]acid-soluble metabolites (ASMs) in the media ( $n = 3$ ). \* $P < 0.05$ . Cont., control.

mutant, indicating the catalytic activity of ACOT1 is necessary for its regulation of FA oxidation and TG turnover. Taken together, these data suggest that *Acot1* knockdown reduces hepatic TG levels through increased TG turnover and enhanced oxidation of both exogenous and endogenous FAs.

### ACOT1 Regulates PPAR $\alpha$ Activity

Because we observed an increase in FA oxidation, we next measured the expression of target genes of PPAR $\alpha$ , the principal transcription factor governing hepatic FA oxidation (7). Surprisingly, *Acot1* knockdown reduced expression of PPAR $\alpha$  and peroxisome proliferator-activated receptor  $\gamma$  coactivator 1 $\alpha$  (PGC1 $\alpha$ ) target genes (Fig. 3*A* and *B*). In addition, catalase protein expression, a marker of peroxisome content, and mitochondrial DNA abundance were reduced with *Acot1* knockdown (Fig. 3*C* and *D*). When combined with the aforementioned effects on FA oxidation,

these results suggest that ACOT1 uncouples FA oxidation from the upregulation of genes and machinery involved in oxidative metabolism.

We next speculated that the overexpression of ACOT1 could drive PPAR $\alpha$  activity. To test this, COS7 cells and L cells were transfected with EV, *Acot1*, or *Acot1*-S232A plasmids and treated with vehicle or 8-Br-cAMP. The combination of 8-Br-cAMP and ACOT1 enhanced PPAR $\alpha$  reporter activity more than 8-Br-cAMP alone in COS7 cells (Fig. 4*A*) and L cells (Fig. 4*B*). Moreover, induction of PPAR $\alpha$  reporter activity by ACOT1 was dependent on its catalytic activity, suggesting that ACOT1 regulates PPAR $\alpha$  through production of FA ligands. *Acot1* knockdown in AML12 cells also blocked the induction of PPAR $\alpha$  target gene expression by 8-Br-cAMP (Supplementary Fig. 8). Together, these data suggest that ACOT1 synergizes with cAMP to promote PPAR $\alpha$  activity.



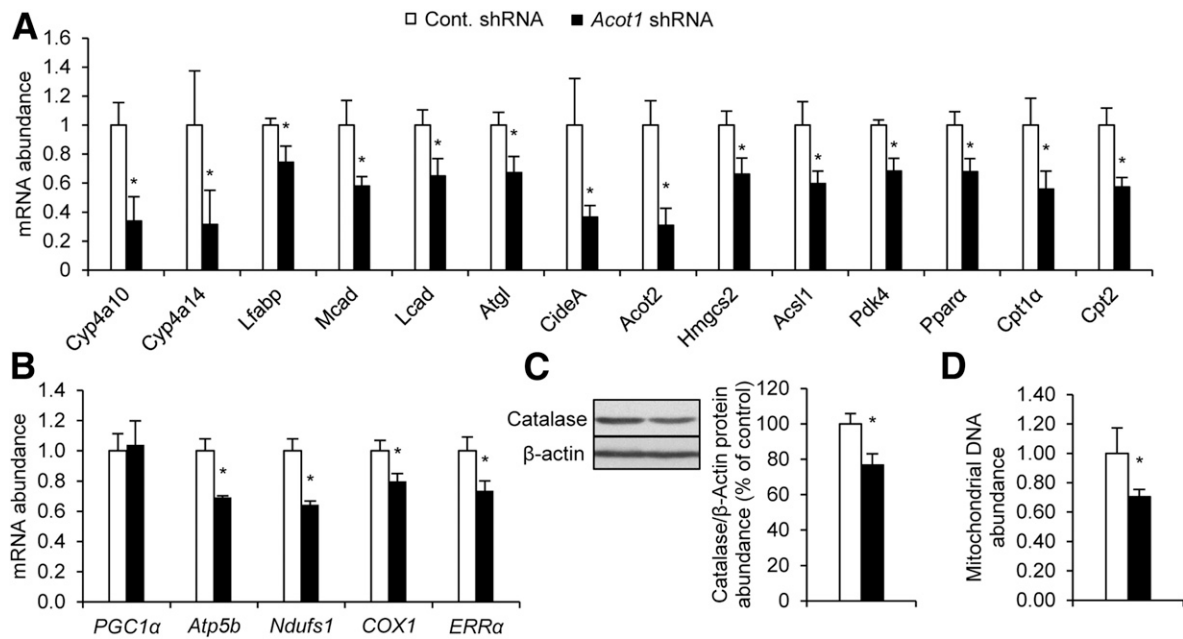


**Figure 3**—ACOT1 regulates expression of PPAR $\alpha$  target genes (A) and PGC1 $\alpha$  target genes (B) was reduced with *Acot1* knockdown ( $n = 7$  mice). C: Expression of catalase protein, a marker of peroxisome abundance, was reduced with *Acot1* knockdown; densitometry represents  $n = 5$  mice. D: Mitochondrial DNA abundance was reduced with *Acot1* knockdown. \* $P < 0.05$ . Cont., control.

### 8-Br-cAMP Promotes ACOT1 Nuclear Translocation

Although characterized as a cytosolic protein, the data in Fig. 1C and D and Supplementary Fig. 2C suggest that ACOT1 is also present in the nucleus. Because ACOT1 has no predicted nuclear localization sequence (26), yet has numerous putative PKA phosphorylation sites (27), we suspected that nuclear location of ACOT1 could be driven by elevated cAMP/PKA signaling during fasting. To test the translocation of ACOT1 under  $\beta$ -adrenergic stimulation, AML12 cells were treated with H89, a PKA inhibitor, for 1 h, followed by 8-Br-cAMP for an additional 10 min before cells were fixed and stained for ACOT1. Nuclear ACOT1 increased with the addition of 8-Br-cAMP; however, this effect was blocked by H89 (Fig. 4C and D). Nuclear localization of ACOT1 was also confirmed in COS7 cells transfected with *Acot1* DsRed-Express N1 treated with vehicle or 8-Br-cAMP (Fig. 4E). An ACOT1 signal was detectable in the nucleus in response to 8-Br-cAMP but not when treated with a vehicle. Together, these data suggest that ACOT1 regulates PPAR $\alpha$  activity in response to cAMP/PKA signaling, potentially because of its nuclear localization and production of local FA ligands.

### ACOT1 Is Important for Mitigating Oxidative Stress Caused by Enhanced FA Oxidation During Fasting

Enhanced FA oxidation can lead to the production of ROS in the electron transport chain, leading to oxidative stress (28). In response to *Acot1* knockdown, we observed enhanced FA oxidation (Fig. 3D) but a reduction in oxidative mechanisms, as indicated by reduced expression of PPAR $\alpha$  targets (Fig. 4A–E). Such effects could lead to

enhanced ROS generation and oxidative stress. In support of this logic, *Acot1* knockdown livers exhibited significantly more ROS than the control livers (Fig. 5A). In addition to increased ROS, *Acot1* knockdown increased the expression of oxidative stress markers heme oxygenase 1 (*Ho-1*) and uncoupling protein 2 (*Ucp2*) (Fig. 5B). Increases in oxidative stress promote inflammation (15), and PPAR $\alpha$  is well documented as important for anti-inflammatory pathways (13,14). Thus, the reduction in PPAR $\alpha$  targets along with increased oxidative stress suggests *Acot1* knockdown could promote inflammation. Indeed, expression was significantly increased for inflammatory markers *Tnfa*, *Cd11c*, *Il-1 $\beta$* , and *F4/80* (Fig. 5C). Consistent with enhanced inflammatory gene expression, Cd45 immunohistochemistry revealed enhanced immune cell infiltration in livers with *Acot1* knockdown (Fig. 5D). Similarly, immune cell infiltration can also be observed in the micrographs of H-E staining (Fig. 3B). These results suggest that ACOT1 mitigates oxidative stress and inflammation during fasting, potentially by enhancing PPAR $\alpha$  activity.

### Effects of *Acot1* Knockdown Can Be Rescued by PPAR $\alpha$ Agonism

To further explore the potential role of ACOT1 in supplying FA ligands for PPAR $\alpha$  activation, we attempted to rescue the effects of ACOT1 knockdown by feeding mice a diet supplemented with a synthetic PPAR $\alpha$  ligand, Wy-14643. Mice were treated with adenovirus as described above and fed a purified diet or a diet supplemented with 0.1% Wy-14643 (29) for 1 week. As expected, Wy-14643

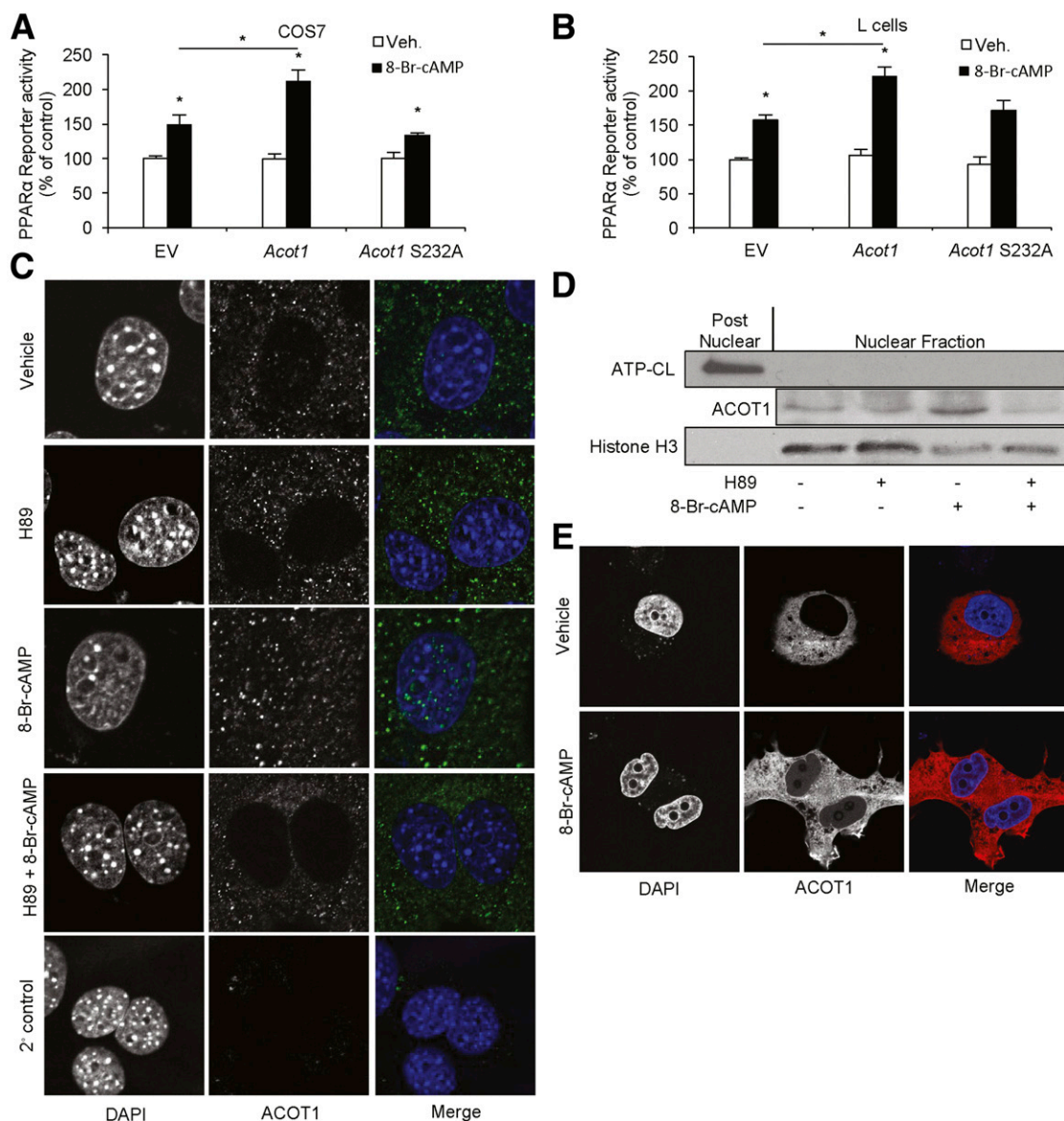


**Figure 4**—ACOT1 regulates PPAR $\alpha$  activity and partially localizes to the nucleus. COS7 cells (A) and L cells (B) were transfected with EV, *Acot1*, or *Acot1*-S232A and reporter assay components ( $n = 6$ –12 wells). Cells were harvested and luciferase activity was assessed. ACOT1 translocates to the nucleus in AML12 cells in response to treatment with 8-Br-cAMP. Pretreatment with H89 blocked the translocation of ACOT1 in response to 8-Br-cAMP, as measured by immunofluorescent staining (C) and nuclear fractionation and Western blotting (D). E: An ACOT1 fusion construct (DsRed) shows partial nuclear localization in response to 8-Br-cAMP in COS7 cells. \* $P < 0.05$ . ATP-CL, ATP-citrate lyase; Veh., vehicle.

significantly increased expression of ACOT1; however, *Acot1* shRNA adenovirus significantly blunted this induction (Fig. 6A). Wy-14643 ablated the effects of *Acot1* knockdown on reducing liver TGs (Fig. 6B and C). However, *Acot1* knockdown and Wy-14643, independently and together, increased TG hydrolase activity (Fig. 6D). As seen above, *Acot1* knockdown increased serum  $\beta$ -hydroxybutyrate in mice fed the control diet, whereas Wy-14643 significantly increased serum  $\beta$ -hydroxybutyrate to a similar level among treatment groups (Fig. 6E). Moreover, Wy-14643 rescued the expression of PPAR $\alpha$  target genes (Fig. 6F) as well as catalase protein expression (Fig. 6G) in mice treated with *Acot1* shRNA. Because Wy-14643 is able to rescue the *Acot1*

knockdown phenotype, ACOT1 is likely responsible for providing FA ligands to activate of PPAR $\alpha$ .

We next explored the possibility that Wy-14643 could also rescue the oxidative stress and inflammation observed in response to *Acot1* knockdown. Wy-14643 was able to normalize the expression of oxidative stress marker *Ho-1* but was unable to normalize *Ucp2* expression in *Acot1* knockdown livers (Fig. 7A). Wy-14643 also normalized the expression of inflammatory genes and prevented immune cell infiltration in livers of *Acot1* knockdown mice (Fig. 7B and C). In summary, these data suggest that ACOT1 regulates PPAR $\alpha$  as a means to influence hepatic energy metabolism, oxidative stress, and inflammation.

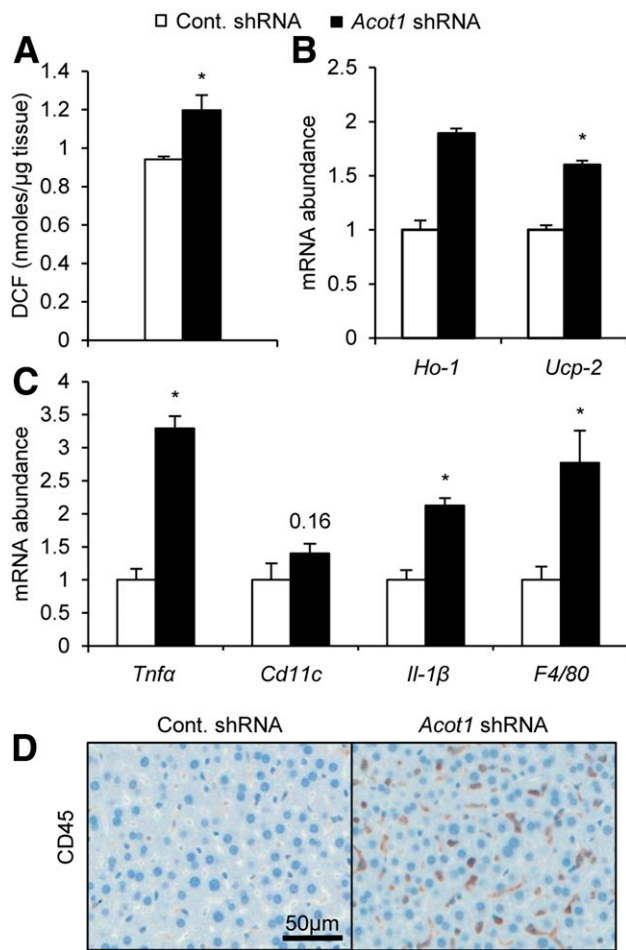


**Figure 5**—Hepatic *Acot1* knockdown increases inflammation and oxidative stress in mice. **A:** *Acot1* knockdown increased intracellular ROS measured by an OxiSelect in vitro ROS/RNS kit ( $n = 4$  mice). **B:** *Acot1* knockdown increased expression of the oxidative stress genes *Ho-1* and *Ucp2*. **C:** Expression of inflammatory markers are increased in mice treated with *Acot1* shRNA ( $n = 7$  mice). **D:** CD45 immunohistochemistry stains from liver tissues revealed increased immune cell infiltration after *Acot1* knockdown ( $n = 2$  mice). \* $P < 0.05$ . Cont., control; DCF, 2',7'-dichlorodihydrofluorescein diacetate.

### Effects of *Acot1* Knockdown in Diet-Induced Steatosis

Because *Acot1* knockdown resulted in oxidative stress and inflammation, both hallmarks of liver disease, we investigated the effects of *Acot1* knockdown in mice fed an HFD. Mice were fed a 45% fat diet for 12 weeks before adenoviral delivery of cont. shRNA or *Acot1* shRNA (Supplementary Fig. 9A and B). Abundant lipid droplet accumulation was observed in livers of mice fed the HFD, but *Acot1* knockdown mice had hepatic TG content similar to that in controls (Supplementary Fig. 9C and D). *Acot1* knockdown increased serum  $\beta$ -hydroxybutyrate (Supplementary Fig. 9E) despite unchanged expression of PPAR $\alpha$  (Supplementary Fig. 9F) or PGC1 $\alpha$  (Supplementary Fig. 9G) target genes. Despite the lack of reductions in gene expression, mitochondrial content was reduced with *Acot1* knockdown (Supplementary Fig. 9H). As expected, *Acot1* knockdown

solicited a robust induction of inflammatory and oxidative stress markers (Supplementary Fig. 9I). *Acot1* knockdown also increased ROS (Supplementary Fig. 9J) and fibrosis (Supplementary Fig. 9K). Together, these data suggest that under HFD-induced steatosis, ACOT1 is protective against the inflammation and oxidative stress that lead to fibrosis.

### DISCUSSION

The liver imports FAs in proportion to their concentration in the blood. Thus, increased rates of FA metabolism must match this uptake during times of fasting. Upon entering the liver, hepatic FAs are first converted to acyl-CoA molecules, before they enter most metabolic pathways (3). ACOT1 catalyzes the reverse reaction, producing free FAs (5), which should slow the flux of FAs to downstream metabolic pathways. Consistent with this logic, hepatic knockdown of ACOT1 increased the oxidation of FAs in vivo and in vitro (Fig. 2) but had no observed effect on TG synthesis or VLDL secretion (Supplementary Fig. 4). Taken together, these results suggest that ACOT1 specifically regulates FAs destined to oxidative pathways, potentially by removing acyl-CoAs as substrates. By slowing FA oxidation, ACOT1 may serve to protect the liver from the detrimental effects of excessive FA oxidation.

PPAR $\alpha$  is a dominant transcription factor in the liver, responsible for the upregulation of genes involved in FA oxidation during fasting (7,30). *Acot1* knockdown led to enhanced FA oxidation, which would be expected to correlate with higher expression of several PPAR $\alpha$  target genes. However, expression of PPAR $\alpha$  targets was reduced (Fig. 3A) following *Acot1* knockdown, despite the greater oxidative rate. Because FAs serve as endogenous ligands to activate PPAR $\alpha$  (10), we speculated that ACOT1 provides FA ligands to activate PPAR $\alpha$ . Therefore, administration of a synthetic PPAR $\alpha$  ligand (e.g., Wy-14643) should rescue the effects of hepatic *Acot1* knockdown on PPAR $\alpha$  signaling. Wy-14643 treatment largely rescued the phenotype resulting from ACOT1 knockdown, including normalization of FA oxidation and PPAR $\alpha$  target genes (Fig. 6). We also tested whether the thioesterase activity of ACOT1 was necessary for its regulation of PPAR $\alpha$ . Expressing ACOT1 in COS7 or L cells increased PPAR $\alpha$  reporter activity during 8-Br-cAMP stimulation. However, a catalytically dead ACOT1 mutant (*Acot1* S232A) had no effect on PPAR $\alpha$  activity compared with the EV (Fig. 4A and B), supporting the theory that ACOT1 thioesterase activity provides FA ligands to regulate PPAR $\alpha$ . Surprisingly, we found no difference in cytosolic or nuclear free FAs with *Acot1* knockdown (Supplementary Fig. 10). Free FAs are lipotoxic substances that are tightly regulated inside cells (1). It is possible that the ACOT1-derived FA pool may be too small or transient to see distinct differences in total quantity, or that FAs are selectively channeled to influence PPAR $\alpha$  activity. ACOT1 overexpression alone was not sufficient to increase PPAR $\alpha$  reporter activity; only during cAMP/PKA signaling did ACOT1 solicit PPAR $\alpha$  activation (Fig. 4A and B). We observed nuclear localization of ACOT1 in response to 8-Br-cAMP (Fig. 4C–E),



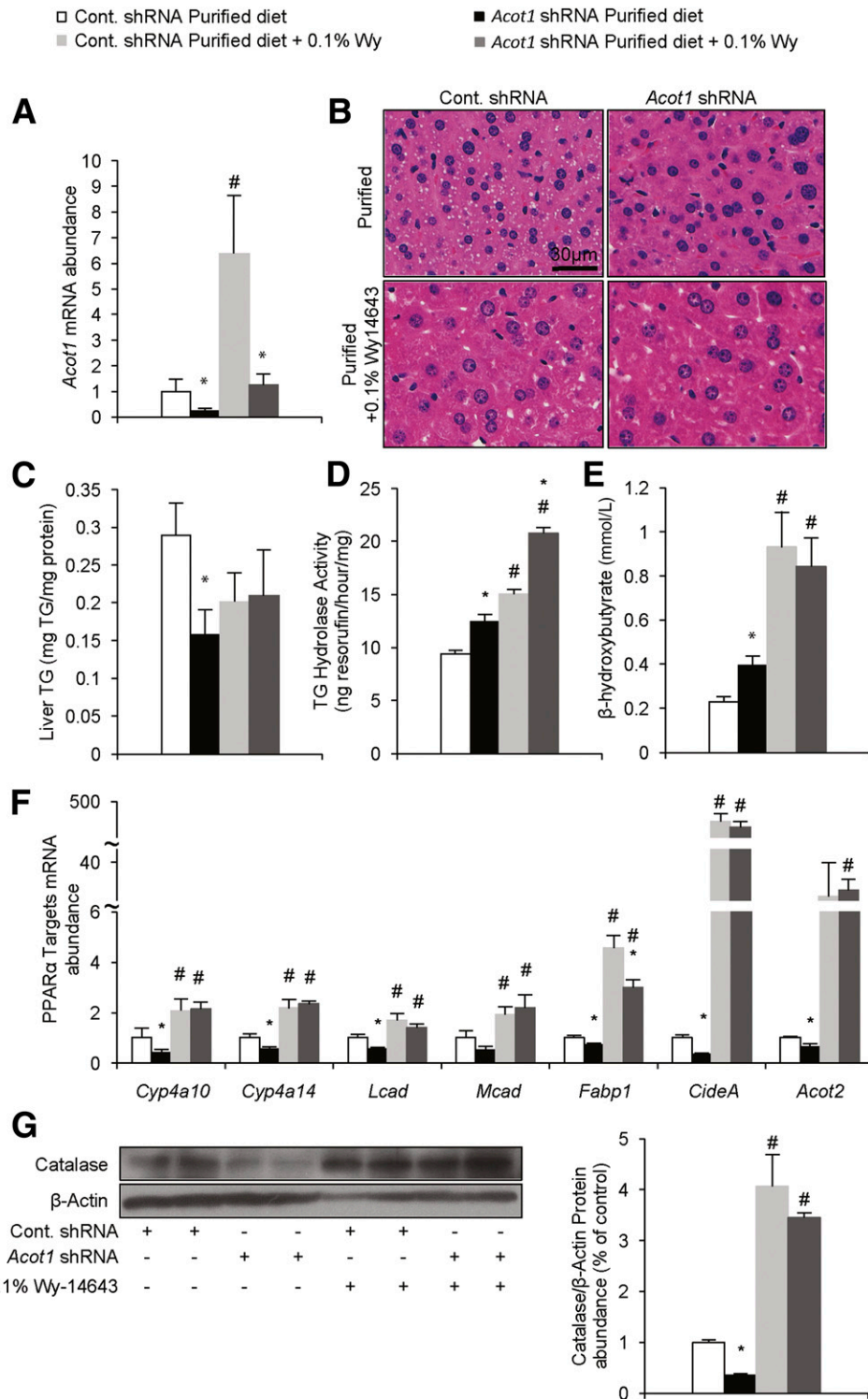


**Figure 6**—Wy-14643 rescues the effects of *Acot1* knockdown. **A:** *Acot1* mRNA after adenovirus treatments and 0.1% Wy-14643 (Wy) supplementation ( $n = 7-9$ ). **B:** H-E staining shows that Wy-14643 reduced and normalized lipid droplet accumulation in the *Acot1* knockdown treatment group. **C:** Wy-14643 normalized liver TG levels between the control and *Acot1* shRNA treatment groups. TG hydrolase activity (**D**) and serum  $\beta$ -hydroxybutyrate concentrations (**E**) are increased and normalized following Wy-14643 supplementation ( $n = 4$  mice). **F:** Wy-14643 increased PPAR $\alpha$  target gene expression and rescued the effects of *Acot1* knockdown. **G:** Catalase protein expression is increased by Wy-14643 and normalized in livers of *Acot1* shRNA-treated mice ( $n = 2$  mice). \* $P < 0.05$  vs. the cont. shRNA group. # $P < 0.05$  vs. the control diet. Cont., control.

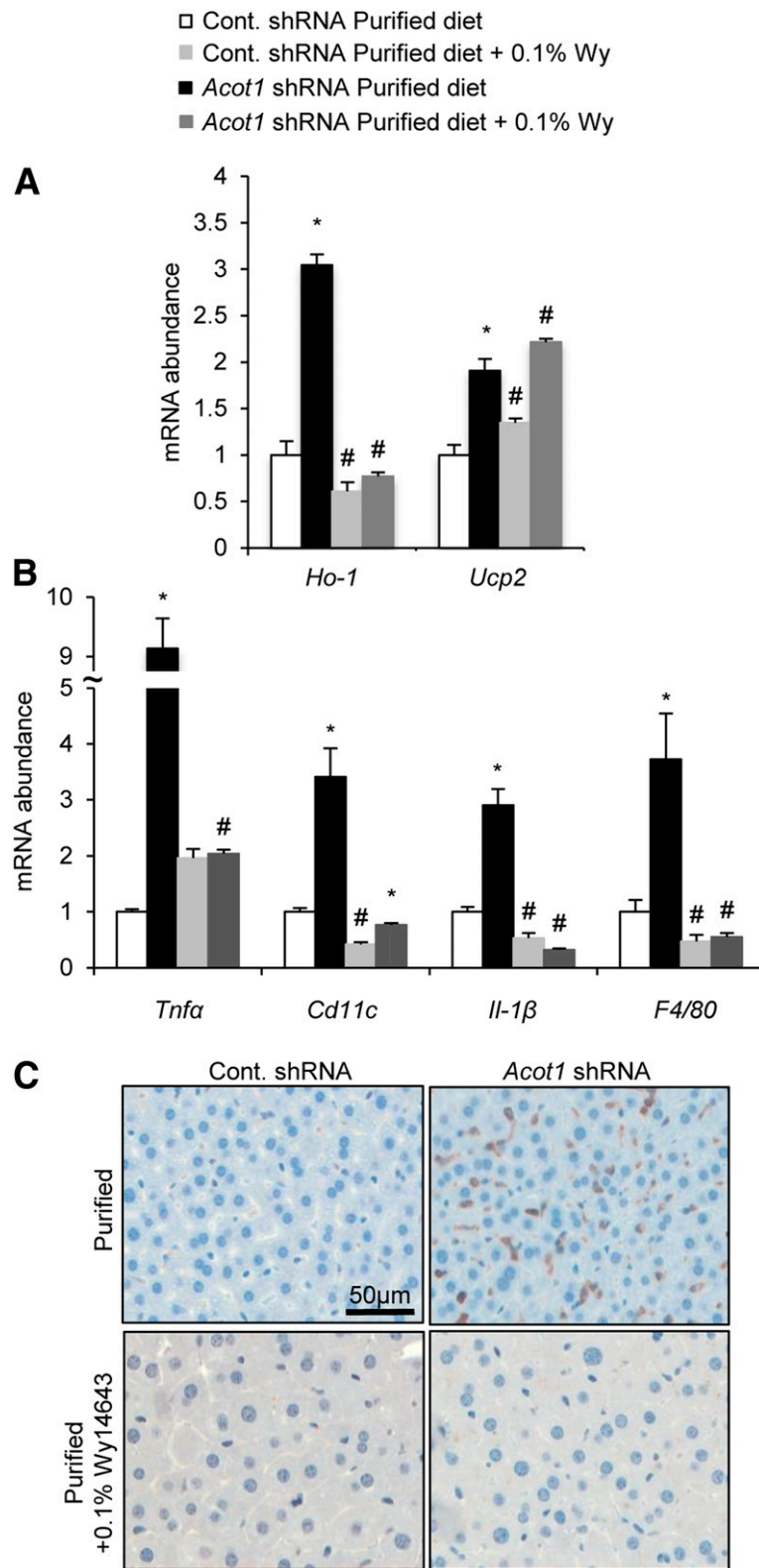


**Figure 7**—Wy-14643 (Wy) rescues inflammation and oxidative stress markers. Wy-14643 normalized the expression of most oxidative stress markers (A) and reduced the inflammatory markers observed with *Acot1* knockdown ( $n = 7-9$  mice) (B). C: Wy-14643 normalized macrophage infiltration assessed by Cd45 immunohistochemistry staining ( $n = 2$  mice). \* $P < 0.05$  vs. the cont. shRNA group. # $P < 0.05$  vs. the purified control diet. Cont., control.

suggesting nuclear localization may be necessary for ACOT1 to activate PPAR $\alpha$ . Similarly, *Acot1* knockdown reduced nuclear ACOT1 (Supplementary Fig. 2C) and subsequently reduced PPAR $\alpha$  transcripts (Fig. 3A). Thus, these data show that ACOT1 produces FA ligands to activate PPAR $\alpha$ , increasing FA oxidative capacity. This regulation may be dependent on the nuclear localization of ACOT1 in response to fasting and cAMP/PKA signaling.

Normal mitochondrial oxidation produces a mild stress on cells, resulting in the production of ROS (15). However, ROS production is balanced by mitochondrial antioxidant activity that protects the mitochondria from oxidative stress. During times of increased FA oxidation, ROS can exceed antioxidant capacity and lead to oxidative stress (31). In addition, PPAR $\alpha$  signaling limits oxidative stress (32,33) and promotes the expression of anti-inflammatory genes (13). Greater hepatic ROS and expression of oxidative stress markers were found in hepatic *Acot1* knockdown mice (Fig. 5A and B); these paralleled elevated rates of FA oxidation (Fig. 2) and reduced PPAR $\alpha$  target gene expression (Fig. 3A). In addition, greater inflammatory gene expression and immune cell infiltration occurred in response to *Acot1* knockdown (Fig. 5C and D). Thus, the inflammation observed in response to *Acot1* knockdown could be the result of reduced PPAR $\alpha$ -dependent anti-inflammatory gene expression. Wy-14643 treatment rescued the oxidative stress and inflammation seen in *Acot1* knockdown livers (Fig. 7). As such, ACOT1 seems to protect the liver from oxidative stress and inflammation via promotion of PPAR $\alpha$  signaling.

Because oxidative stress and inflammation are key events in the progression of nonalcoholic fatty liver disease (34), perhaps it is not surprising that *Acot1* knockdown increased oxidative stress and inflammation, ultimately leading to

fibrosis in response to high-fat feeding. Current evidence suggests that HFDs increase FA oxidation (35), which correlates with the increase in serum  $\beta$ -hydroxybutyrate we observed in mice fed an HFD (Supplementary Fig. 8E) compared with basal mice (Fig. 2D). This increase in FA oxidation is associated with the oxidative stress and inflammation that occur as the disease progresses (36). Our findings support the importance of FA oxidation and its complications in promoting the progression of nonalcoholic fatty liver disease from steatosis to fibrosis and implicate ACOT1 as playing an important role in balancing FA oxidation, ROS, and inflammation.

To our knowledge, this is the first study to characterize the physiological importance of ACOT1 in hepatic fasting lipid metabolism. This study highlights a significant role for ACOT1 in regulating FA oxidation, PPAR $\alpha$  activity, oxidative stress, and inflammation during fasting. In support of a protective role for ACOT1, humans with fewer copy numbers of the 14q24.3 locus, where ACOT1 resides, are more likely to develop nonalcoholic steatohepatitis, a disease in which oxidative stress and inflammation are the defining characteristics (37). Similarly, overexpression of ACOT1 improves diabetic cardiomyopathy by reducing FA oxidation and ROS production (19). Thus, when combined, the few studies evaluating ACOT1 all highlight a potential beneficial role of ACOT1 in mitigating the negative effects of aberrant lipid metabolism.

Based on our current findings, ACOT1 plays a pivotal role in protecting livers from excess FA oxidation and the ensuing oxidative stress and inflammation, while simultaneously promoting PPAR $\alpha$  activity (Fig. 8). In addition, ACOT1 locates to the nucleus during fasting, suggesting a potential local regulation of PPAR $\alpha$  via the production of FA ligands. Thus, this work highlights the importance of

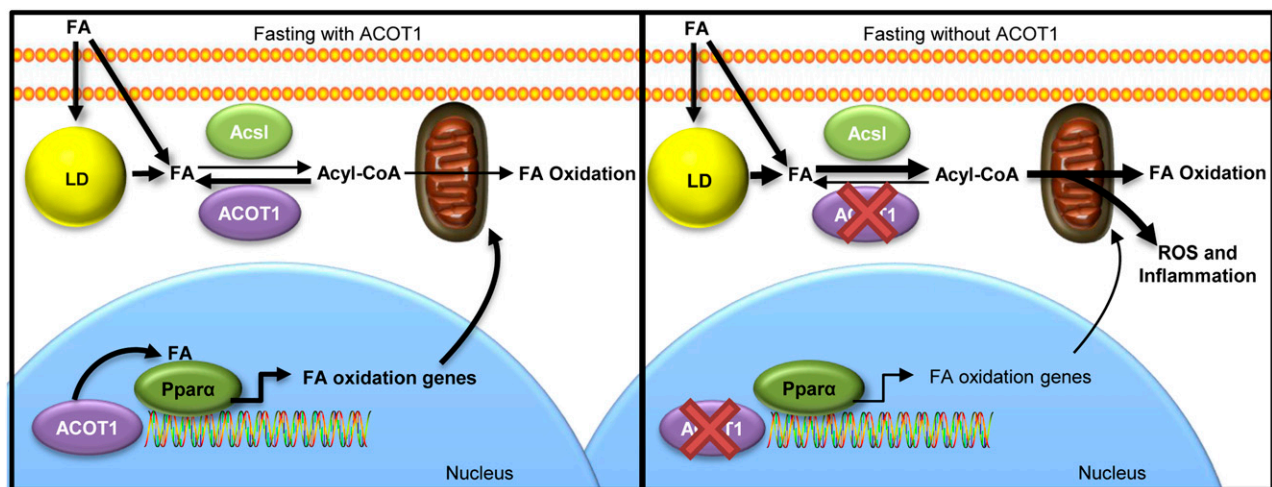


**Figure 8**—Proposed mechanism of ACOT1 in fasting lipid metabolism in the liver. ACOT1 expression during fasting mitigates FA flux toward oxidation in the cytosol. Under fasting and with elevated cAMP/PKA stimulation, nuclear ACOT1 is important in the activation of PPAR $\alpha$ . Fasting with reduced ACOT1 enhances FA oxidation and reduces PPAR $\alpha$  activity, which lead to oxidative stress and inflammation. Therefore, ACOT1 is an important enzyme for balancing oxidative capacity, oxidative stress, and inflammation with PPAR $\alpha$  activity during fasting. *Acs1*, long-chain acyl-CoA synthetase; LD, lipid droplet.

ACOT1 as a branch point in regulating FA flux to oxidative pathways and controlling the transcriptional regulation of FA oxidation.

**Acknowledgments.** The authors thank Mara Mashek (University of Minnesota) for her technical training and support.

**Funding.** This study was supported by a National Institutes of Health/National Institute of Diabetes and Digestive and Kidney Diseases T32 Training grant, Minnesota Obesity Training Program Predoctoral Fellowship (DK083250 to M.P.F.).

**Duality of Interest.** No potential conflicts of interest relevant to this article were reported.

**Author Contributions.** M.P.F. designed and performed most of the experiments, wrote the manuscript, and contributed to the discussion. A.S. performed some of the experiments. D.G.M. designed and oversaw all of the experiments and edited the manuscript. D.G.M. is the guarantor of this work and, as such, had full access to all the data in the study and takes responsibility for the integrity of the data and the accuracy of the data analysis.

**Prior Presentation.** Parts of this study were presented in abstract form at the Annual Meeting of Experimental Biology, Chicago, IL, 22–26 April 2017.

## References

- Nguyen P, Leray V, Diez M, et al. Liver lipid metabolism. *J Anim Physiol Anim Nutr (Berl)* 2008;92:272–283
- Coleman RA, Mashek DG. Mammalian triacylglycerol metabolism: synthesis, lipolysis, and signaling. *Chem Rev* 2011;111:6359–6386
- Mashek DG, Li LO, Coleman RA. Long-chain acyl-CoA synthetases and fatty acid channeling. *Future Lipidol* 2007;2:465–476
- Hunt MC, Alexson SEH. The role Acyl-CoA thioesterases play in mediating intracellular lipid metabolism. *Prog Lipid Res* 2002;41:99–130
- Yamada J, Sakuma M, Ikeda T, Fukuda K, Suga T. Characteristics of dehydroepiandrosterone as a peroxisome proliferator. *Biochim Biophys Acta* 1991;1092:233–243
- Hunt MC, Lindquist PJ, Peters JM, Gonzalez FJ, Diczfalussy U, Alexson SE. Involvement of the peroxisome proliferator-activated receptor alpha in regulating long-chain acyl-CoA thioesterases. *J Lipid Res* 2000;41:814–823
- Montagner A, Polizzi A, Fouché E, et al. Liver PPAR $\alpha$  is crucial for whole-body fatty acid homeostasis and is protective against NAFLD. *Gut* 2016;65:1201–1214
- Hunt M, Lindquist PJ, Nousiainen S, Svensson TL, Diczfalussy U, Alexson SE. Cloning and regulation of peroxisome proliferator-induced acyl-CoA thioesterases from mouse liver. *Adv Exp Med Biol* 1999;466:195–200
- Huhtinen K, O'Byrne J, Lindquist PJG, Contreras JA, Alexson SEH. The peroxisome proliferator-induced cytosolic type I acyl-CoA thioesterase (CTE-I) is a serine-histidine-aspartic acid alpha/beta hydrolase. *J Biol Chem* 2002;277:3424–3432
- Nakamura MT, Yudell BE, Loo JJ. Regulation of energy metabolism by long-chain fatty acids. *Prog Lipid Res* 2014;53:124–144
- Forman BM, Chen J, Evans RM. Hypolipidemic drugs, polyunsaturated fatty acids, and eicosanoids are ligands for peroxisome proliferator-activated receptors alpha and delta. *Proc Natl Acad Sci U S A* 1997;94:4312–4317
- Chakravarthy MV, Lodhi IJ, Yin L, et al. Identification of a physiologically relevant endogenous ligand for PPARalpha in liver. *Cell* 2009;138:476–488
- Gervois P, Kleemann R, Pilon A, et al. Global suppression of IL-6-induced acute phase response gene expression after chronic in vivo treatment with the peroxisome proliferator-activated receptor- $\alpha$  activator fenofibrate. *J Biol Chem* 2004;279:16154–16160
- Wahli W, Michalik L. PPARs at the crossroads of lipid signaling and inflammation. *Trends Endocrinol Metab* 2012;23:351–363
- García-Ruiz C, Colell A, Morales A, Kaplowitz N, Fernández-Checa JC. Role of oxidative stress generated from the mitochondrial electron transport chain and mitochondrial glutathione status in loss of mitochondrial function and activation of transcription factor nuclear factor-kappa B: studies with isolated mitochondria and rat hepatocytes. *Mol Pharmacol* 1995;48:825–834
- Belhadj Slimen I, Najjar T, Ghram A, Dabbebi H, Ben Mrad M, Abdrabbah M. Reactive oxygen species, heat stress and oxidative-induced mitochondrial damage. A review. *Int J Hyperthermia* 2014;30:513–523
- Brookes PS. Mitochondrial H(+) leak and ROS generation: an odd couple. *Free Radic Biol Med* 2005;38:12–23
- Murphy MP. How mitochondria produce reactive oxygen species. *Biochem J* 2009;417:1–13
- Yang S, Chen C, Wang H, et al. Protective effects of acyl-coA thioesterase 1 on diabetic heart via PPAR $\alpha$ /PGC1 $\alpha$  signaling. *PLoS One* 2012;7:e50376
- Ong KT, Mashek MT, Bu SY, Greenberg AS, Mashek DG. Adipose triglyceride lipase is a major hepatic lipase that regulates triacylglycerol turnover and fatty acid signaling and partitioning. *Hepatology* 2011;53:116–126
- Schrammel A, Mussbacher M, Wölkart G, Stessel H, Pail K, Winkler S, et al. Endothelial dysfunction in adipose triglyceride lipase deficiency. *Biochim Biophys Acta* 2014;1841:906–917.
- Bu SY, Mashek MT, Mashek DG. Suppression of long chain acyl-CoA synthetase 3 decreases hepatic de novo fatty acid synthesis through decreased transcriptional activity. *J Biol Chem* 2009;284:30474–30483
- Moffat C, Bhatia L, Nguyen T, et al. Acyl-CoA thioesterase-2 facilitates mitochondrial fatty acid oxidation in the liver. *J Lipid Res* 2014;55:2458–2470
- Kirkby B, Roman N, Kobe B, Kellie S, Forwood JK. Functional and structural properties of mammalian acyl-coenzyme A thioesterases. *Prog Lipid Res* 2010;49:366–377
- Ohtomo T, Nakao C, Sumiya M, et al. Identification of acyl-CoA thioesterase in mouse mesenteric lymph nodes. *Biol Pharm Bull* 2013;36:866–871
- Kosugi S, Hasebe M, Tomita M, Yanagawa H. Systematic identification of cell cycle-dependent yeast nucleocytoplasmic shuttling proteins by prediction of composite motifs. *Proc Natl Acad Sci U S A* 2009;106:10171–10176
- Huttlin EL, Jedrychowski MP, Elias JE, et al. A tissue-specific atlas of mouse protein phosphorylation and expression. *Cell* 2010;143:1174–1189
- Atlante A, Calissano P, Bobba A, Azzariti A, Marra E, Passarella S. Cytochrome c is released from mitochondria in a reactive oxygen species (ROS)-dependent fashion and can operate as a ROS scavenger and as a respiratory substrate in cerebellar neurons undergoing excitotoxic death. *J Biol Chem* 2000;275:37159–37166
- Wölkart G, Schrammel A, Dörrfel K, Haemmerle G, Zechner R, Mayer B. Cardiac dysfunction in adipose triglyceride lipase deficiency: treatment with a PPAR $\alpha$  agonist. *Br J Pharmacol* 2012;165:380–389
- Pawlak M, Lefebvre P, Staels B. Molecular mechanism of PPAR $\alpha$  action and its impact on lipid metabolism, inflammation and fibrosis in non-alcoholic fatty liver disease. *J Hepatol* 2015;62:720–733
- Day CP, James OF. Steatohepatitis: a tale of two “hits”? *Gastroenterology* 1998;114:842–845
- Abdelmegeed MA, Moon K-H, Hardwick JP, Gonzalez FJ, Song B-J. Role of peroxisome proliferator-activated receptor-alpha in fasting-mediated oxidative stress. *Free Radic Biol Med* 2009;47:767–778
- Yoo SH, Park O, Henderson LE, Abdelmegeed MA, Moon K-H, Song B-J. Lack of PPAR $\alpha$  exacerbates lipopolysaccharide-induced liver toxicity through STAT1 inflammatory signaling and increased oxidative/nitrosative stress. *Toxicol Lett* 2011;202:23–29
- Koo S-H. Nonalcoholic fatty liver disease: molecular mechanisms for the hepatic steatosis. *Clin Mol Hepatol* 2013;19:210–215
- Sunny NE, Satapati S, Fu X, et al. Progressive adaptation of hepatic ketogenesis in mice fed a high-fat diet. *Am J Physiol Endocrinol Metab* 2010;298:E1226–E1235
- Satapati S, Kucejova B, Duarte JAG, et al. Mitochondrial metabolism mediates oxidative stress and inflammation in fatty liver. *J Clin Invest* 2015;125:4447–4462
- Zain SM, Mohamed R, Cooper DN, et al. Genome-wide analysis of copy number variation identifies candidate gene loci associated with the progression of non-alcoholic fatty liver disease. *PLoS One* 2014;9:e95604